Powder characterization using X-ray tomography and image analysis

Bernier, Fabrice; Pelletier, Roger; Lefebvre, Louis-Philippe

Advances in Powder Metallurgy & Particulate Materials: 2016: Proceedings of the 2016 International Conference on Powder Metallurgy & Particulate Materials Sponsored by the Metal Powder Industries Federation, June 5-8, 2016, 2016-06-

Powder Characterization Using X-ray Tomography and Image Analysis

Fabrice Bernier, Roger Pelletier, Louis-Philippe Lefebvre
National Research Council Canada
Boucherville, Qc, J4B 6Y4, Canada

Korbinian Heim
Technische Universität Berlin
Berlin, D-16023, Germany

ABSTRACT

Large scale deployment of additive manufacturing (AM) processes relies on part quality, specifically the presence of internal defects and part-to-part consistency. Some of the defects observed in finished parts have been associated with porosities in the powder feedstock used in AM processes including powder bed, laser cladding, and cold spray. Since the level of porosity in these powders is generally very low, standard characterization techniques, such as pycnometry and metallography with image analysis, are not well suited for quantification. This study presents a new approach combining high resolution X-ray tomography with 3D image analysis to evaluate and quantify porosity in titanium powder feedstock. The effects of acquisition parameters and image analysis procedures on porosity quantification were investigated to validate the proposed method and assess its reliability. Data demonstrates that the proposed technique is sufficiently sensitive to differentiate powders with different porosity levels.

INTRODUCTION

In the additive manufacturing (AM) process, loose metallic particles are fused together using high energy focused heat sources, such as high power laser or electron beam to build a component layer by layer. Defects in an AM part can originate from the building process[1-2] as a result of the lack of powder fusion, or the defect can already be present in the powder feedstock itself, i.e. trapped gas.[3-4] The porosity in the powder can be easily observed using different techniques, but is difficult to quantify since the volume fraction is generally very low.

Standard porosity characterization methods such as light optical metallography (LOM) and pycnometry have major limitations. Pycnometry gives a precise measurement of the powder density, from which the porosity content can be calculated, but it does not offer information on the shape and size of the pores. Also, this technique is mostly limited to pure metals due to the difficulty in precisely assessing the

theoretical density of the alloy. Indeed, theoretical densities are known for alloys having a defined constituent content and alloys are usually specified within compositional ranges. Thus, each powder batch may have compositions slightly different from each other and the effect of this variation on the density may be of the same order of magnitude as the effect of the internal porosity. Consequently, it is difficult to discriminate the effect of the internal porosity from the variation of the theoretical density of the alloy. Standard metallographic techniques allow obtaining high resolution images. When combined with image analysis tools, they provide accurate quantification of 2D features. However, they do not allow adequate statistical evaluation of 3D features. Also, careful sample preparation is required to avoid polishing artefacts such as smearing.

Recently, X-ray computed tomography (XCT) has been used as a non-destructive technique to observe 3D defects obtained during electron beam melting additive manufacturing.[5-6] Furthermore, Léonard et al. assessed the porosity in a Ti6Al4V powder feedstock using XCT.[4] They measured a pore fraction of 0.09% with a mean diameter of 12.1 µm for a powder having a size distribution between 45 to 100 µm. XCT, while being a very powerful technique, still possesses limitations: spatial resolution depends on part size, has lower resolution than scanning electron microscopy, and creates large datasets leading to high computational time for analysis.[7]

This paper focuses on describing how XCT parameters and image analysis routine affect the quantification of porosity in titanium powders. In order to demonstrate the capacity and source of errors, porosity of two titanium powders have been measured and compared with other standard techniques.

EXPERIMENTAL PROCEDURES

Table I presents the two titanium powders used for this study. Pure titanium was chosen to minimise the uncertainty associated with the measurement of porosity measured using gas pycnometry (i.e. evaluation of the theoretical density of the dense metal).

Table I: Description of powder feedstock used in this study.

Sample	Production Process	Theoretical density (g/cm^3)	Particle size distribution by volume (µm)		
			D_{10}	D_{50}	D_{90}
Ti-1	Plasma atomised	4.507	55	76	103
Ti-2	Gas atomised	4.507	37	98	179

For the XCT measurement, samples of the different powders were embedded in an epoxy resin and machined into 3.175mm diameter cylindrical specimens to obtain a fixed volume and to be as close as possible to the X-ray source and achieve maximal resolution (3 µm). The measurements were made using a Nikon HMXST 225 computed tomography system with a minimal focal spot size of 3 µm and using a Perkin-Elmer 1621 AN amorphous silicon flat panel (409.6 x 409.6 mm) coupled with a CsI scintillator detector. The main operating conditions for the different powders are shown in Table II.

Table II: Acquisition conditions and parameters of the XCT.

Material	X-ray source voltage (kV)	X-ray source current (μA)	Filter	Exposure time (ms)	Number of projections
Titanium	135	64	0.5 mm Cu	1000	3142

An image analysis routine for the 3D reconstructed XCT volume was built using Image J software.

The powder densities were determined using a Helium gas pycnometer (Micromeritics). Light-optical metallographic observations were done on as-polished samples at 200X magnification and quantification was carried out using a Clemex Vision image analysis system. Particle size analyses were made by laser diffraction using a Beckman Coulter LS13 320 apparatus.

RESULTS AND DISCUSSION

The first step for the quantification of the level of porosity is to obtain a high quality image, i.e. a high resolution and high contrast image. The selection of optimal parameters for image analysis was done with the Ti-1 powder.

Effect of the number of average frames and filter on contrast

The contrast between the metal and the void (or resin) should be high enough to enable a clear segmentation of the image based on grey thresholding. One way to increase the contrast without modifying the key acquisition parameters, stated in Table II, is to average several images taken for each projection. Figure 1 compares the obtained results when a single image is used compared to an average of 8 frames; the impact on the grey value scales is also shown. One of the first steps during the image analysis routine was to use a median filter to increase phase distinction. The impact of the filter on the images and grey values is presented in Figure 2.

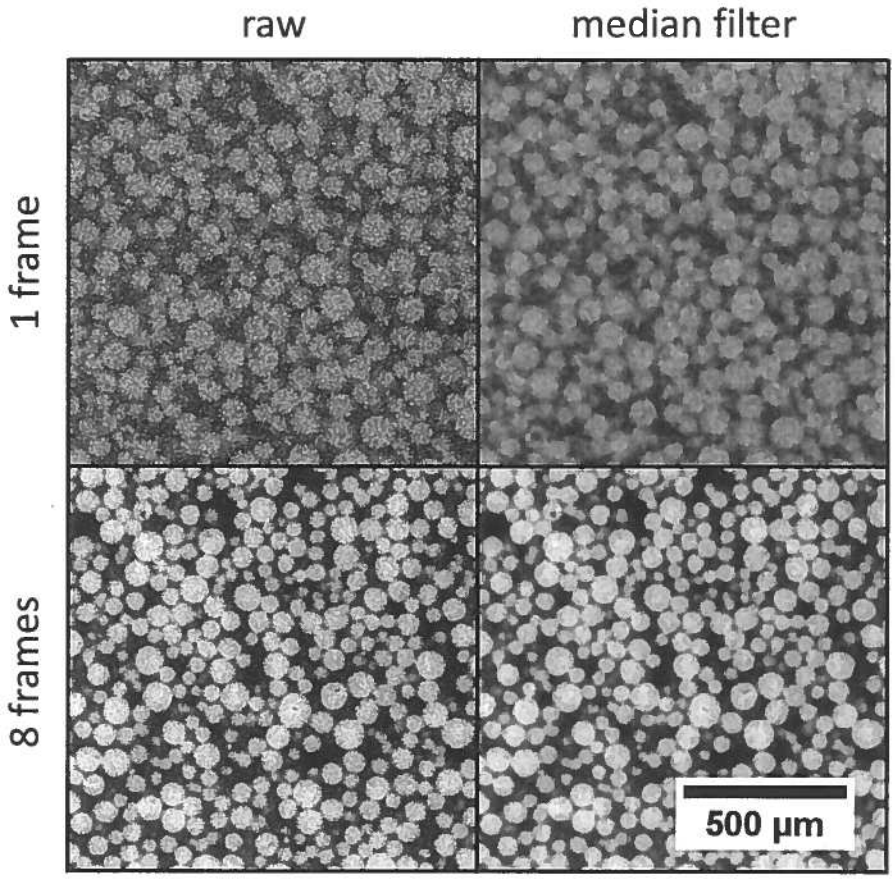

Figure 1. Impact of frame averaging for Ti-1 on the treated images

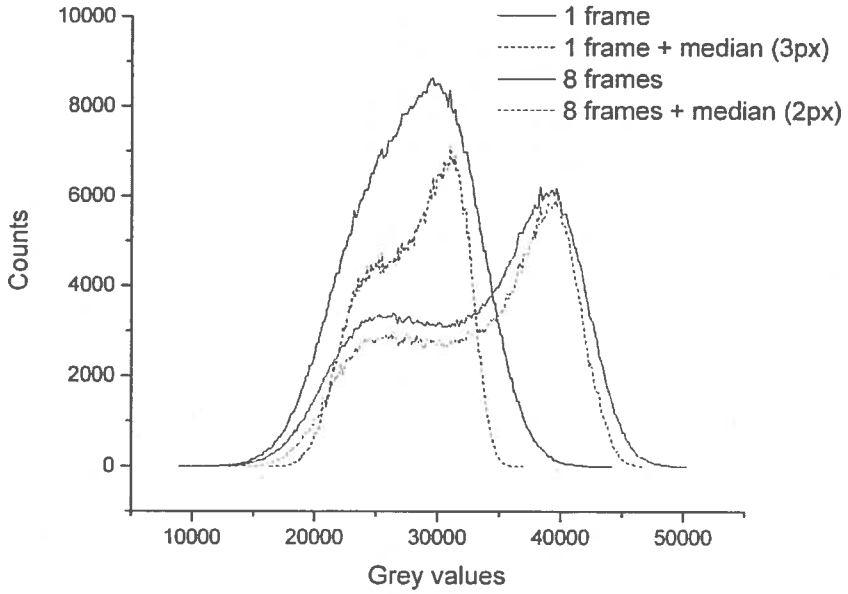

Figure 2. Impact of frame averaging for Ti-1 on the grey values spectrum

A clear distinction between the two peaks of the grey values is only obtained when averaging 8 frames. The median filter on the single frame image enables peak separation, but the peaks are not as distinct compared to the 8 frames averaging. The impact of frame averaging on the measurements of the particle and pore size is illustrated in Figure 3. There is no major difference on the quantification of the particle size diameter, but the D_{50} of the pore size nearly doubles when the 8 frames averaging is used. Based on the visual inspection of the 3D reconstructions, the description of pore sizes using the 8 frames averaging is more accurate. For this reason, 8 frames averaging was used for the remainder of the study to ensure quantification quality. It should be noted that the scanning acquisition time is proportional to the number of frames used during the scan.

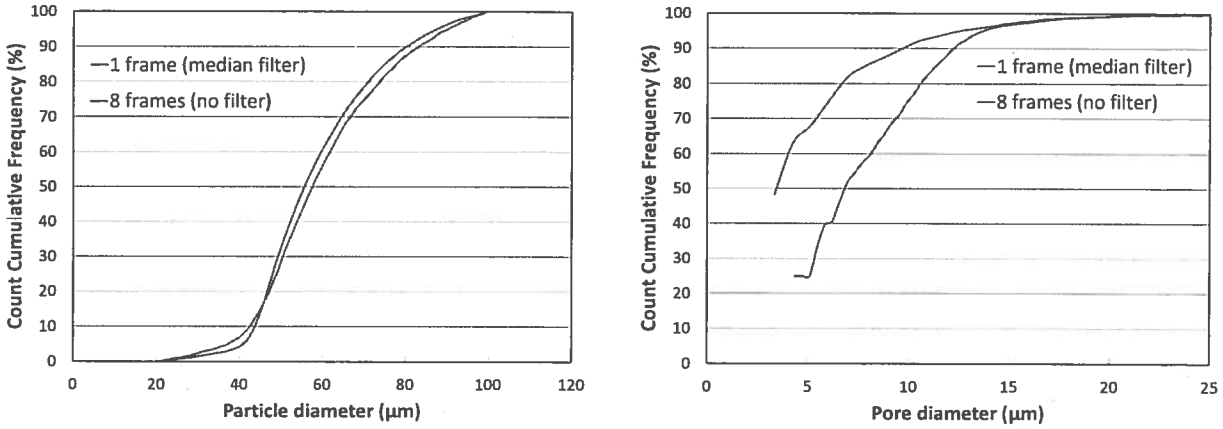

(a) (b)

Figure 3. Impact of frames averaging for Ti-1 on the quantification of (a) particle size distribution and of (b) pore size distribution.

Effect of resolution

Another crucial factor to obtain a high quality image is spatial resolution, which is expressed in terms of voxel size (volume of one cubic pixel). For all three acquisition conditions listed in Table II, the focal spot size was under 3 µm. However, in order to achieve a 3 µm voxel size, the magnification must also be high. With the type of equipment used in this study, increasing the magnification is obtained by moving the samples closer to the X-ray source, thus increasing the projection surface on the panel detector (Figure 4). However, this leads to a reduction of the scanned volume. Table III summarizes the magnification and analyzed volume (assuming a cylindrical sample) for a given voxel size.

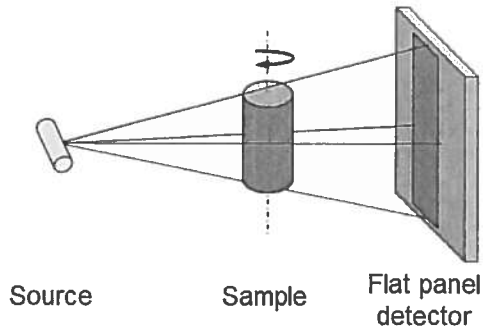

Figure 4. Schematic of sample positioning and magnification.

Table III: Relation between voxel size and analyzed volume.

Voxel size (µm)	Position from the source (mm)	Magnification	Analyze volume (mm^3)
3	8	65.3 X	170
5	19	40.2 X	785
10	49	54 X	6283

The impact of the reconstruction voxel size on the images for the same analyzed region is shown in Figure 5. While only a small difference in image sharpness can be seen between the 3 µm and the 10 µm voxel sizes, the image analysis routine was not able to adequately analyse the 10 µm images without the use of a median filter and a lot of artefacts (powder merging) were generated. This is even more apparent on the particle segmentation results (Figure 6).

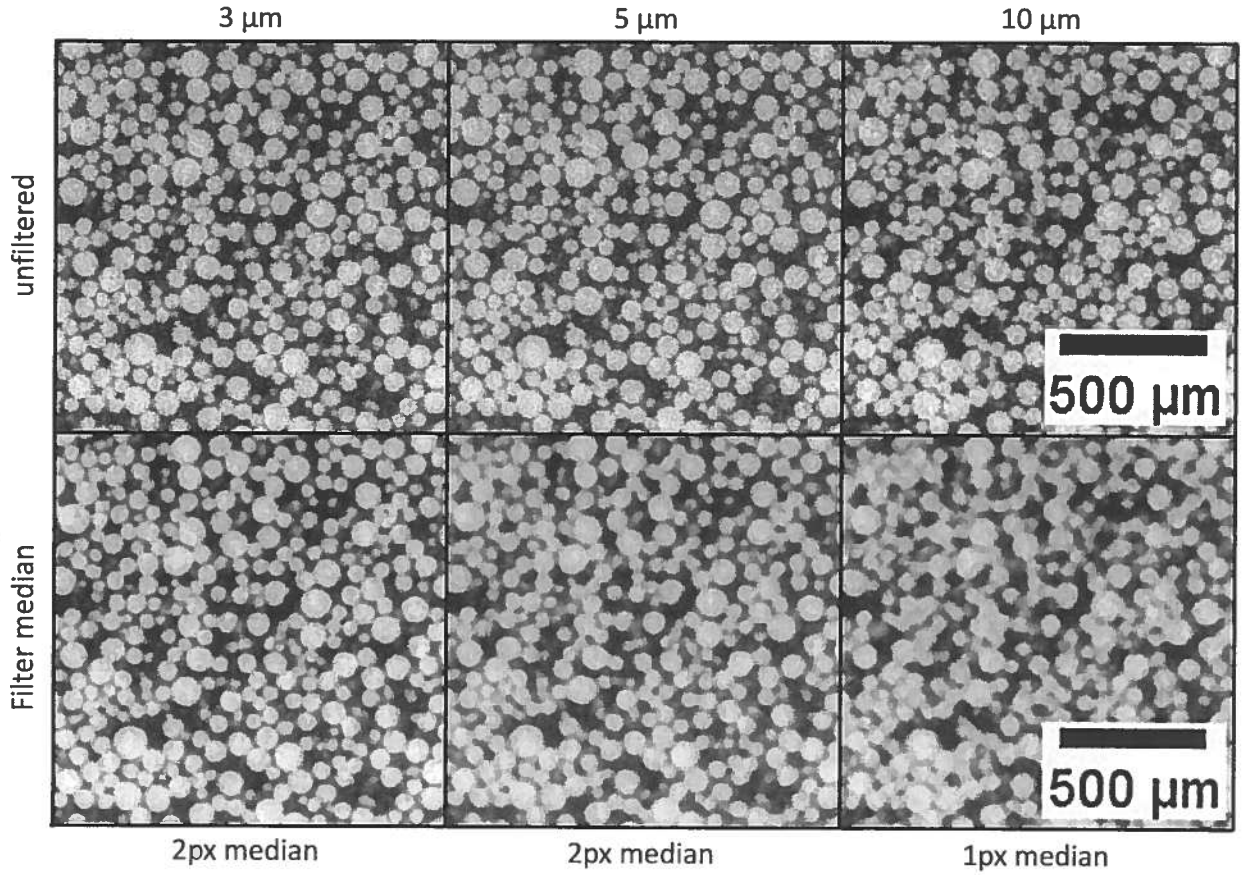

Figure 5. Influence of voxel size and median filtering on image quality.

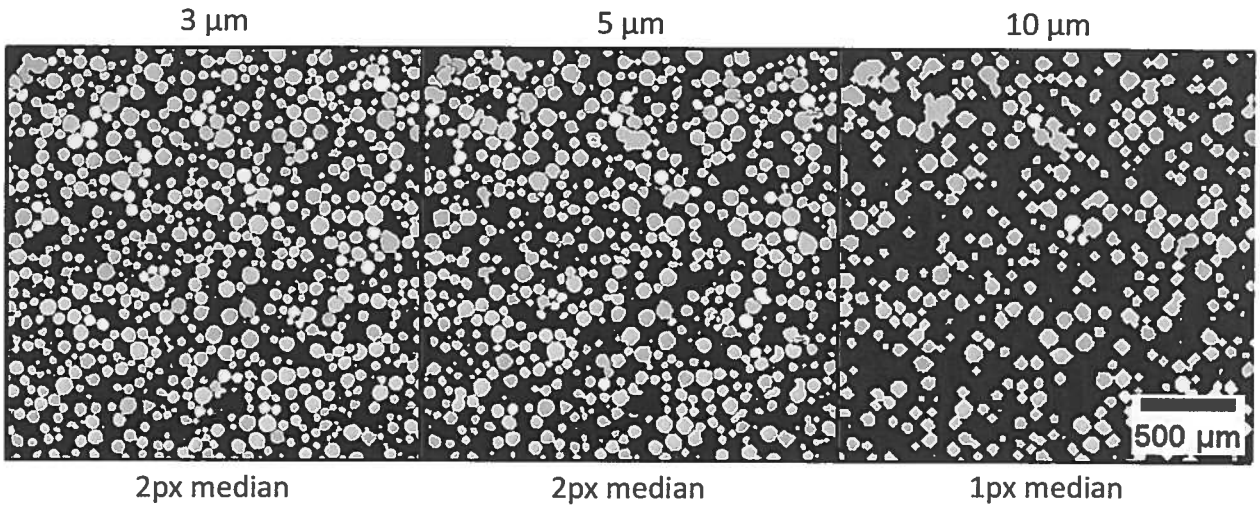

Figure 6. Influence of voxel size on particle segmentation.

The segmentation process yields similar results when we compare the 3 and 5 µm voxel size images (Figure 6). However, when the results from the image analysis routines are compared (Figure 7), it is clear that scanning with a resolution of 10 microns is not enough for the Ti-1 powder. A voxel size of 3 or 5 µm leads to similar particle size distributions, while pore size distribution varies significantly with voxel size.

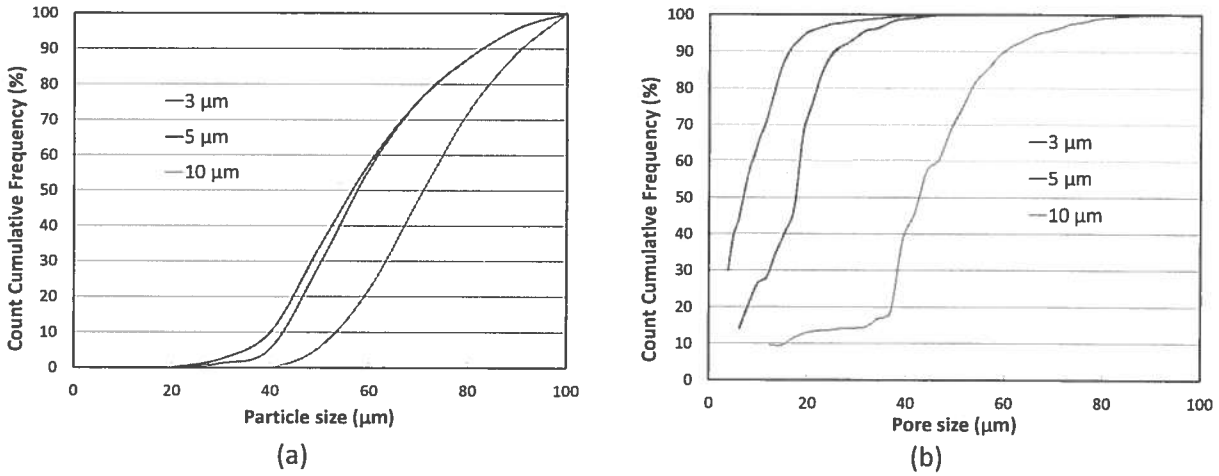

Figure 7. Influence of voxel size on (a) particle size and (b) pore size for Ti-1.

Validation of acquisition parameters with other techniques

In order to evaluate the reliability of the XCT, the results were compared with those obtained using other characterization techniques. Figure 8 illustrates the image analysis routine carried out on an optical photomicrograph of a polished cross-section of Ti-1 powder at a magnification of 200X. Particles that were cut off from the process frame and those that were too close to each other to be counted individually by the image analysis routine (see the three particles in the middle right of Figure 8 (b))

were not analyzed. More than 75 fields were analyzed and the spherical diameter was calculated from the 2D images using the following equation (Clemex Vision PE user's guide):

$$Spherical\ Diameter = Mean\ Chord \times 1.27324 \times 1.2247$$

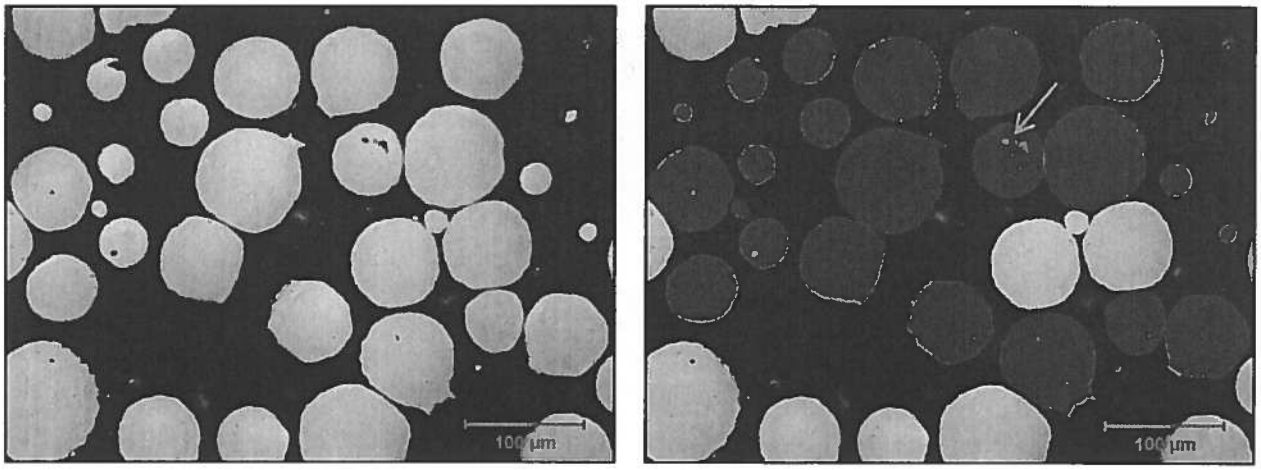

(a) (b)

Figure 8. Optical photomicrograph (a) and results of image analysis routine (b) for powder feedstock Ti-1.

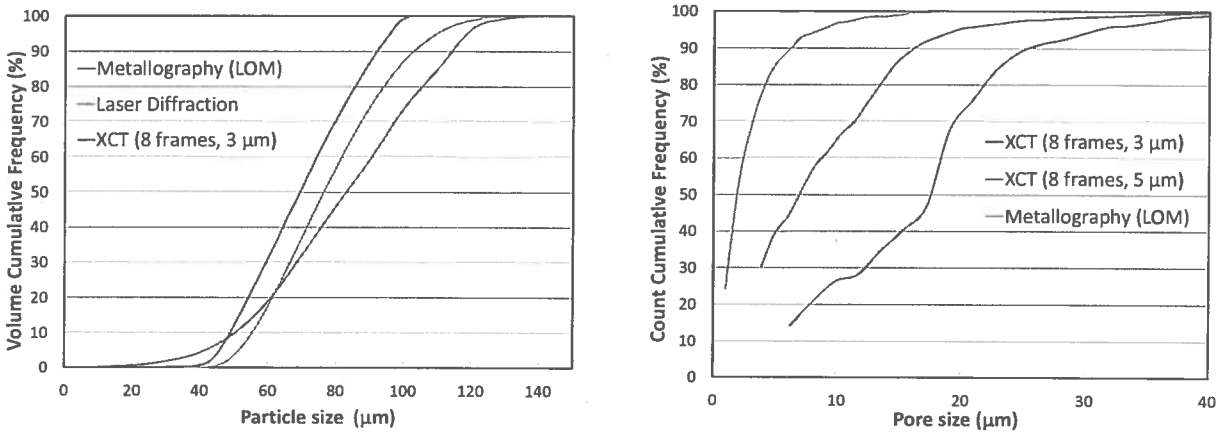

(a) (b)

Figure 9. Comparison of XCT and other methods for the quantification of (a) particle size and (b) pore size for Ti-1.

The comparison between the results obtained with the different techniques is shown in Figure 9. In the case of the particle size distribution, it is observed that XCT tends to slightly underestimate particle size when compared to laser diffraction, while light optical metallography seems to overestimate it. Indeed, D_{50} values of spherical diameter are 68.7, 76.4 and 82.9 µm for XCT, laser diffraction and metallography (LOM), respectively. For pore size distribution, it is clear that the XCT method neglects pore sizes lower than the voxel size, which explains most of the difference observed between XCT and LOM results. Hence, when assessing pore size distribution, the XCT scan should be done at the highest possible magnification at the expense of sample size. Also, during a 2D analysis, some pores may be counted

individually while they may in fact be interconnected, as seen in Figure 8 (b) for the three small pores indicated by the green arrow. This could explain the lower count of larger pores obtained by LOM analysis.

Another crucial powder characteristic for powder producers and part manufacturers alike is the presence of pores inside particles and the quantification of their volume fraction. When comparing the XCT results to those obtained by pycnometry and LOM (Table IV) for powder Ti-1, it is difficult to determine which technique is the most reliable since the level of porosity is very low. Hence the comparison analysis was extended to powder Ti-2, which is known to be more porous. Here the XCT analysis was carried out on two samples to evaluate reproducibility, thus explaining the large number of analyzed pores. These results clearly suggest that XCT is a valuable technique to evaluate pore content and that it can be used for quality control purposes on powder feedstocks.

Table IV: Comparison of pore content obtained from XCT, pycnometry and LOM.

Sample	Gas Pycnometry			XCT (number of analyzed pores)		LOM (number of analyzed pores)
	Theoretical density (g/cm^3)	Measured density (g/cm^3)	Porosity	3 µm	5 µm	
Ti-1	4.507	4.499±0.002	0.17%	0.053% (2444)	0.055% (705)	0.078% (223)
Ti-2	4.507	4.486±0.002	0.47%	0.424%±0.035% (14999)	-	0.68% (124)

CONCLUSION

X-ray computed tomography combined with image analysis was used to characterize titanium powders. The effect of acquisition parameters and sample size on contrast and resolution and their impact on the measured porosity was assessed. The use of 8 frames averaging, to the detriment of acquisition time, and of 3 µm voxel, at the expense of sample size, yield high quality images which enable the 3D quantification of particle and pore sizes, as well as pore content in the powder particles. The results were compared with those obtained using three standard characterization techniques (laser diffraction, light optical metallography and pycnometry) to assess the reliability of the technique. It is clear that this XCT combined with image analysis offers many advantages. A better understanding of its strengths and limitations can make it a powerful tool for quality control of powder feedstocks.

REFERENCE

1. H. Gu, H. Gong, J.J.S. Dilip, D. Pal, A. Hicks, H. Doak and B. Stucker, "Effects of Powder Variation on the Microstructure and Tensile Strength of Ti-6Al-4V Parts Fabricated by Selective Laser Melting", *Int. J. of Powder Metall.*, 2015, vol .51, no.1, pp. 35-42.

2. A. du Plessis, S.G. le Roux, J. Els, G. Booysen and D.C. Blaine, "Application of microCT to the non-destructive testing of an additive manufactured titanium component", *Case Studies in Nondestructive Testing and Evaluation*, 2015, vol. 4, pp. 1-7.

3. X. Gong, J. Lydon, K. Cooper and K. Chou, "Characterization of Ti-6Al-4V Powder in Electron Beam Melting Additive Manufacturing', *Int. J. of Powder Metall.*, 2015, vol .51, no.1, pp. 25-34.

4. F. Léonard, S. Tammas-Williams, I. Todd, "CT for additive Manufacturing Process Characterisation: Assessment of melt strategies on defect population", *6th Conference on Industrial Computed Tomography*, 2016, Wels, Austria, pp.1-8.

5. S. Tammas-Williams, P.J. Withers, I. Todd and P.B. Prangnell, "The Effectiveness of Hot Isostatic Pressing for Closing Porosity in Titanium Parts Manufactured by Selective Electron Beam Melting", *Metall. and Mater. Trans. A.*, 2016, Article in press, DOI: 10.1007/s11661-016-3429-3.

6. E. Hernandez-Nava, C.J. Smith, F. Derguti, S. Tammas-Williams, F. Leonard, P.J. Withers, I. Todd and R. Goodall, "The Effect of Defects on the Mechanical Response of Ti-6Al-4V Cubic Lattice Structures Fabricated by Electron Bean Melting", *Acta Materialia*, 2016, vol. 108, pp. 279-292.

7. E. Maire and P.J. Withers, "Quantitative X-ray Tomography", *Int. Mater. Reviews*, vol.59, no. 1, pp.1-43.